RSC Advances

PAPER

View Article Online
View Journal | View Issue

Cite this: *RSC Adv.*, 2023, **13**, 7780

Revealing the origin of PL evolution of InSe flake induced by laser irradiation†

Jing Wang, ‡[a] Xiaofei Yue,‡[a] JunQiang Zhu,[a] Laigui Hu, [a] Ran Liu,[a] Chunxiao Cong*[ab] and Zhi-Jun Qiu*[a]

Two-dimensional InSe has been considered as a promising candidate for novel optoelectronic devices owing to large electron mobility and a near-infrared optical band gap. However, its widespread applications suffer from environmental instability. A lot of theoretical studies on the degradation mechanism of InSe have been reported whereas the experimental proofs are few. Meanwhile, the role of the extrinsic environment is still obscure during the degradation. As a common technique of studying the degradation mechanism of 2D materials, laser irradiation exhibits many unique advantages, such as being fast, convenient, and offering *in situ* compatibility. Here, we have developed a laser-treated method, which involves performing repeated measurements at the same point while monitoring the evolution of the resulting PL, to systematically study the photo-induced degradation process of InSe. Interestingly, we observe different evolution behavior of PL intensity under weak irradiation and strong irradiation. Our experimental results indicate the vacancy passivation and degrading effect simultaneously occurring in InSe under a weak laser irradiation, resulting in the PL increasing first and then decreasing during the measurement. Meanwhile we also notice that the passivation has a stronger effect on the PL than the degrading effect of weak oxidation. In contrast, under a strong laser irradiation, the InSe suffers serious destruction caused by excess heating and intense oxidation. This leads to a direct decrease of PL and corresponding oxidative products. Our work provides a reliable experimental supplement to the photo oxidation study of InSe and opens up a new avenue to regulate the PL of InSe.

Received 16th January 2023
Accepted 1st March 2023

DOI: 10.1039/d3ra00324h

rsc.li/rsc-advances

1. Introduction

The advent of semiconducting two-dimensional (2D) layered materials with a broad range of electronic and optical properties has provided fascinating opportunities to design and configure next-generation electronic and photoelectronic devices, such as field-effect transistors, photocatalysts, gas sensors, devices for energy storage and conversion and photodetectors over the past decade.[1–5] Indium selenide (InSe), a recently emerging layered metal monochalcogenide III–VI compound with each InSe layer composed of covalently bonded Se–In–In–Se atomic planes, has received widespread attention, owing to its outstanding carrier mobilities and large-scale tunable bandgap (~1.28–1.8 eV) in a small varying thickness range (2–8L).[6,7] At the same time, the direct bandgap characteristic of multilayer InSe is different from other 2D materials, such as transition metal dichalcogenides (TMDs), which presents a promising candidate for broadband photodetection applications with large absorbance, such as near-infrared photodetection.[6–8]

The optical and electronic properties of InSe are easily affected by the surrounding environment, which restricts its practical applications. Recently, the degradation characteristics of the InSe have been widely studied and many theoretical simulations provided in-depth insights into the degradation mechanism of InSe[9–14] whereas a comprehensive experimental result is still lacking. As a common technique, laser irradiation with good regional selectivity and convenience has been regarded as an effective tool to study the degradation process of 2D materials while it has also been demonstrated to realize the modulation of PL for TMDs.[15–17] Among these studies, most found that laser irradiation can cause the structural degradation and lead to a decline of PL,[18] but the obvious increase of PL has also been observed in other reports.[19] The reasons for the different evolution of PL induced by laser irradiation still need to be explored. On the other hand, long-time laser irradiation may result in heat accumulation on the surface of materials, thus the practical experimental results will suffer an influence from the distinct heat dissipation especially for the materials with bad environment stability. In order to avoid the influence from long-time irradiation adopted in previous reports,[15,16,20] we developed a modified laser treated technique that the photo-

[a]*State Key Laboratory of ASIC & System, School of Information Science and Technology, Fudan University, Shanghai 200433, China. E-mail: zjqiu@fudan.edu.cn*
[b]*Yiwu Research Institute of Fudan University, Yiwu City 322000, Zhejiang, China*

† Electronic supplementary information (ESI) available. See DOI: https://doi.org/10.1039/d3ra00324h

‡ These authors contributed equally to this work.

ablating and PL measurement can be simultaneously achieved by repeating measurements at the same point.

In this work, we report a detailed investigation on the degradation process of InSe under laser irradiation by monitoring its PL intensity evolution. We notice the distinct behaviours that the PL intensity increases first and then decreases for weak irradiation while constantly decreasing under strong irradiation. Here, the vacancy passivation can account for the improvement of PL intensity and the degrading effect induced by oxidation is responsible for the decline. Thus, the initial enhancement behaviour can be attributed to the greater impact on PL from Se vacancy passivation caused by photo-induced gas adsorption (*i.e.* H_2O and O_2), in comparison to the degrading effect induced by laser irradiation. Besides, a faster saturation is observed for the vacancy passivation, which results in the subsequent decrease of PL. Interestingly, a direct decrease of PL is noticed under a strong laser irradiation where the InSe suffers a more serious destruction caused by excess heating and intense oxidation.

2. Experimental

2.1 Measurements and characterizations

The InSe flakes were firstly mechanically exfoliated onto polydimethylsiloxane film (PDMS) from the bulk crystal of InSe (HQ graphene company) and then deposited onto SiO_2/Si substrates with a 300 nm SiO_2 layer. The InSe atomic flakes were roughly identified by optical contrast and then the thickness of each layer was characterized by atomic force microscopy (AFM) in non-contact mode under ambient conditions. The Raman spectra were obtained by 1800 lines per mm grating while 150 lines per mm for PL spectra through a confocal Raman system (WITec Alpha300 R) with 532 nm laser wavelength. An objective lens of 100× magnification and 0.95 numerical aperture (NA) was used, and the spot size is ~500 nm in diameter. Argon (Ar) plasma was used to treat InSe for varying durations at different powers at room temperature. PL and Raman spectra were measured immediately after plasma treatment. In addition, we keep the same InSe flake in different spots for the experiments shown in Fig. 2, 3 and 4 and a new flake of the same thickness in Fig. 5.

In vacuum measurements, the samples were mounted in the chamber of a refrigeration system (CRYO Industries of America, Inc.) at room temperature, the sample chamber was evacuated to a high vacuum of greater than 10^{-6} mbar throughout the experiment.

2.2 Modified laser treated technique

We designed the developed technique to avoid the effects of heat caused by prolonged exposure to laser irradiation on a sample previously reported.[15,16,20] We sequentially measured the Raman/PL spectrum of InSe flakes by increasing the number of measurements. The time gap between each measurement was 3 s. For each measurement the acquisition time for the Raman/PL spectrum was 3 s, and twice accumulated. Laser power was either 0.2 or 2 mW.

3. Results and discussion

3.1 Basic characterization

The exfoliated InSe flakes were transferred onto a SiO_2/Si substrate through micromechanical exfoliation technique. Fig. 1a shows the optical image of the InSe flakes whose thickness was identified by mean of the optical contrast and further verified by atomic force microscopy (AFM) as shown in Fig. 1b. Fig. 1c presents the stack Raman spectra of InSe with different thicknesses under an excited laser energy of 2.33 eV. A few representative Raman peaks located at ~115, ~178, ~196, and ~228 cm^{-1} are observed, corresponding to the vibration modes of $A_1(\Gamma_1^2)$, $E(\Gamma_3^1)$-LO, $A_1(\Gamma_1^1)$-TO, and $A_1(\Gamma_1^3)$ respectively, in good agreement with the previous reports.[21–23] It is noted that the bulk sample exhibits all prominent Raman characteristics whereas almost disappears as the thickness down to 2L, stemming from the suppressed interlayer coupling. Fig. 1d shows the corresponding PL spectrum with an obvious decrease of intensity as the thickness decreases from bulk to 2L, which is mainly dominated by a major change in the electronic band structure, possibly a direct-to-indirect bandgap transition caused by quantum confinement, as observed in InSe nanoparticles.[24] Meanwhile, a significant blueshift of the emission energy is noticed which is consistent with the evolution of a bandgap of InSe that gradually shifts from ~1.28 eV (bulk) to ~1.8 eV (bilayer).[6,7,25]

The crystal quality of exfoliated bulk InSe is characterized by PL as shown in Fig S1.† The PL spectra of the bulk InSe flake during repeated measurement are recorded in Fig. 2. Interestingly, the PL intensity firstly increases and then gradually decreases under the irradiation of 0.2 mW (Fig. 2a). Such photo-induced enhancement behavior was observed in some TMDs as well.[15,16] Therein, two reasonable deductions have been proposed: one is the conversion from trion to exciton induced by the doping effect of physical molecule adsorption[26] and the other is that the electrons possess a higher binding energy when localized at the oxygen functional groups formed by chemical reactions, thus suppressing the thermal activation of excitons to auger non-radiative recombination.[17] On the other hand, the decline of PL is generally considered to be the deterioration of structure.[15,16] However, most studies on the PL evolution of InSe induced by laser mainly concentrate on the theoretical simulation, and an experimental result is eagerly needed. Here, we deduce that the photo-induced molecule adsorption may contribute to the main enhancement of PL intensity for InSe with an unavoidable destruction which results in the subsequent decrease (details will be discussed later). Meanwhile, we also notice a direct decrease of PL intensity when InSe are exposed to a 2 mW laser power (Fig. 2b), which may originate from a serious damage of structure.

3.2 Influence factors on PL evolution

In order to explore the influence factors on the variations of PL intensity with increasing measurements, we monitor the InSe degradation process under different conditions as shown in Fig. S2.† We first extract the corresponding PL intensity under

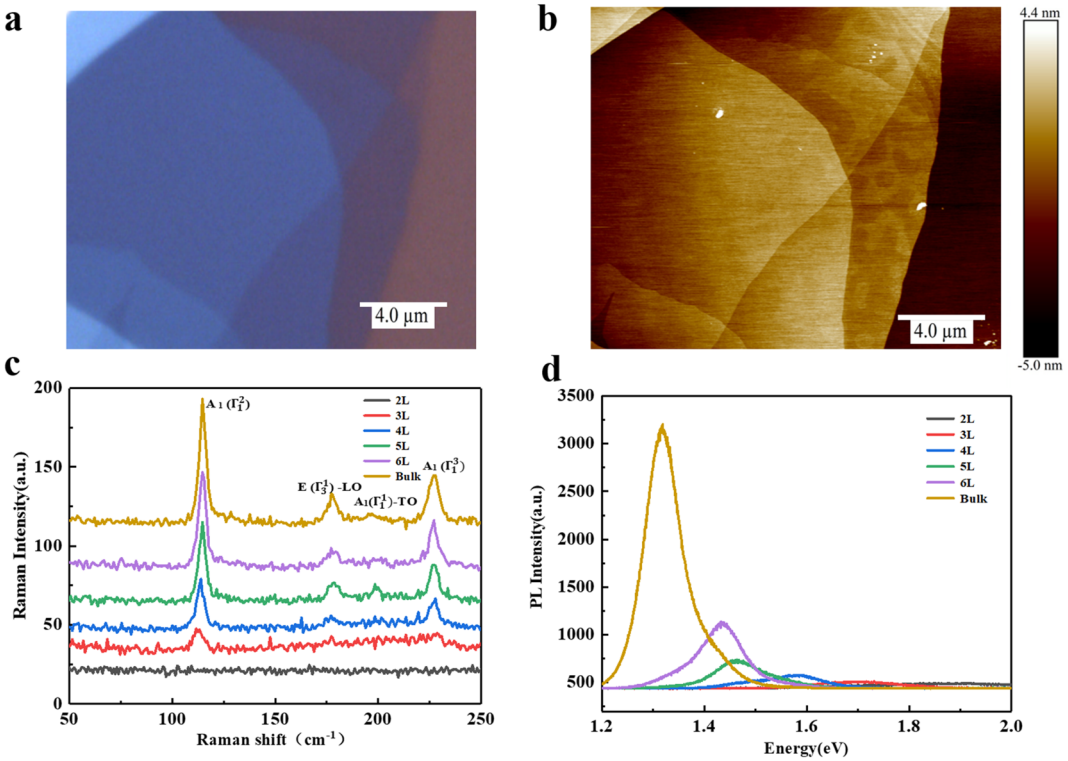

Fig. 1 (a) Optical image of the InSe flake exfoliated onto a SiO_2 (300 nm)/Si substrate with different thickness. (b) The AFM images of as-exfoliated InSe. Scale bar, 4 μm (c) Raman spectra of InSe flakes with different thickness. (d) PL spectra of InSe flakes with different thickness.

different laser power by fitting mixed Lorentz and Gauss functions, as shown in Fig. 3a and b, respectively. In air, the PL intensity firstly increases to the maximum value at measurement no. 8 and then gradually decreases, whereas the PL intensity almost keeps constant under the vacuum condition, which suggests the ambient atmosphere is essential for the increase/decrease of PL. Here, the H_2O and O_2 may play a crucial role according to the previous reports.[16,17,27] In order to verify the deduction, we first perform a laser pre-treatment for the InSe with the expectation of introducing a little absorbent (*i.e.* O_2 and H_2O) and then repeat the test in vacuum. As expected, the PL undergoes a small rise and subsequently stays

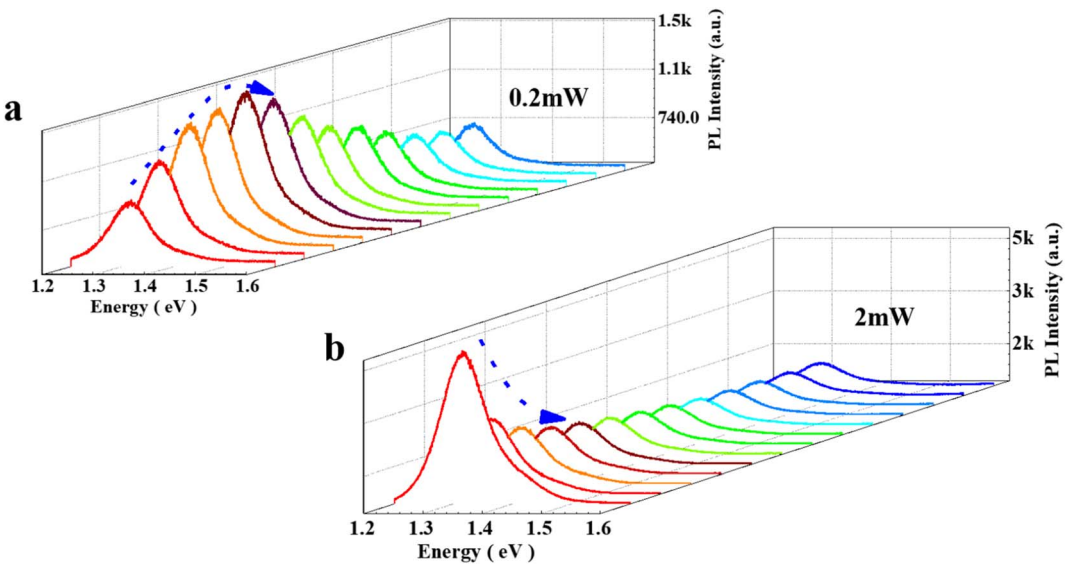

Fig. 2 (a) PL spectra of the bulk InSe under 0.2 mW during repeated measurement. (b) PL spectra of the bulk InSe under 2 mW during repeated measurement.

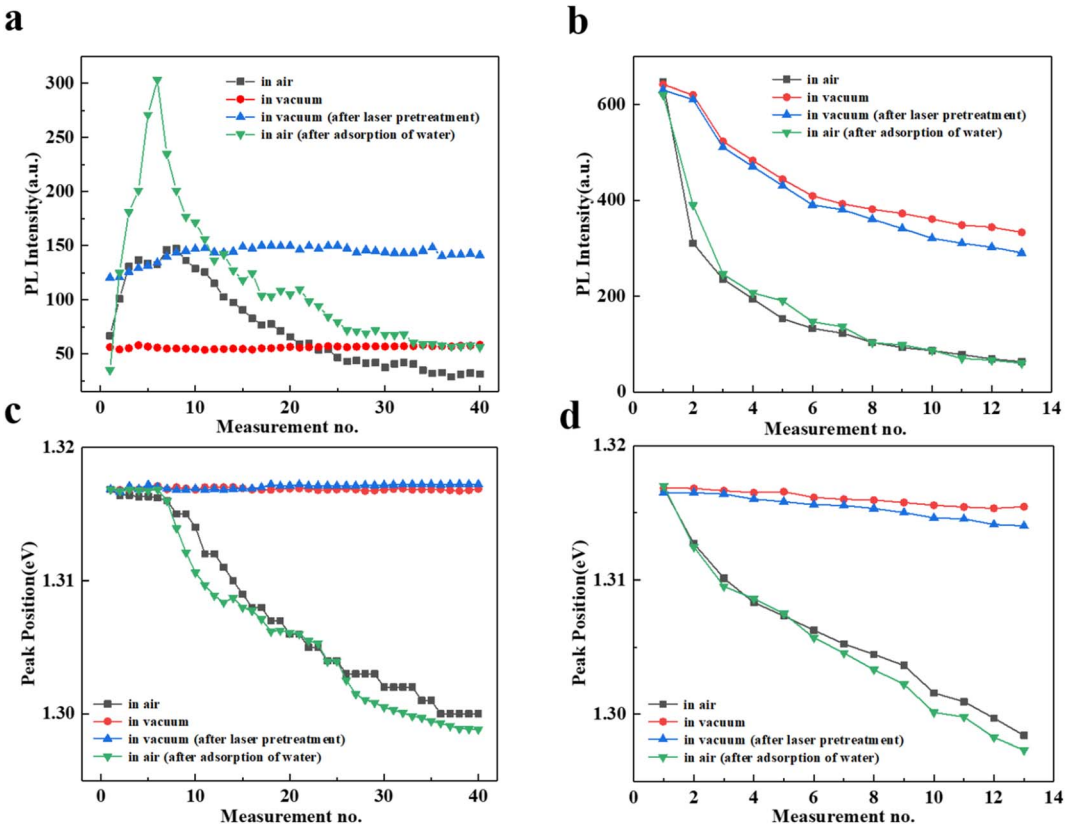

Fig. 3 (a) The PL intensity and position (c) as a function of measurement numbers (No.) under 0.2 mW laser power in different conditions. (b) The PL intensity and position (d) as a function of measurement numbers (No.) under 2 mW laser power in different conditions.

the same with increasing measurements, indicating the introduced adsorbents are rapidly exhausted. These results observed in vacuum condition demonstrate that the unremitting participation of O_2 is required whether the PL enhanced or suppressed. On the other hand, we also observe the strongest PL enhancement in air when we immerse the sample in water to obtain a water-rich InSe. To further understand the interaction between O_2 and H_2O, Fig. S3† presents a control experiment that the water-rich InSe shows a lager PL enhancement compared with the untreated InSe in air, whereas merely leaves a slight PL increasement in vacuum. Interestingly, a reversible process with a comparable enhancement factor for PL is observed when the sample recovers to ambient condition. The results indicate that the H_2O plays a primary role for the enhancement of PL while the O_2 can not absent. In a word, the cooperation between H_2O and O_2 under the laser illumination is required to support the enhancement process. The possible process is that the partial oxidization on InSe surface increases its hydrophilicity, which can promote the adsorption of H_2O according to the previous calculations.[10] The specific mechanism will be discussed later.

Fig. 3b shows the evolution of PL under 2 mW irradiation that the same rapid declines at these four different conditions, indicating the InSe could be directly damaged by heating effect even without O_2 at a higher power. The smaller decreases in these vacuum conditions are probably due to the absence of oxidation process to avoid a more serious damage. Such behaviors are different from the one at low power (0.2 mW), thus we can speculate that both the strong oxidation and heating effect contributing to the damage of InSe at high power, whereas only a degrading effect exists, causing by oxidation for low power. Notably, we also find that the decrease of PL is a self-limiting process, which may result from the saturation of oxidation process.[28]

Fig. 3c and d depict the evolution of extracted peak position of PL *versus* measurement no. under different power. In vacuum, there is no change in peak position for the 0.2 mW irradiation, however a redshift is noticed when the power increases to 2 mW which results from the heating effect, consistent with the change of PL intensity. In air, the peak positions slightly redshift during the process of PL enhancement and then redshift visibly in the stage of decline under the irradiation of 0.2 mW. For 2 mW irradiation, an almost linear redshift in peak position is observed. These results indicate that the structural damage induced by laser may come from the accumulation of minor degradation for a weak irradiation of 0.2 mW. However, the severer structure damage of InSe flakes exposing to a high power can be attributed to the combination of heating effect and a strong oxidation process accompanying with oxide formation, which also supports above results of PL intensity.

It is known that the *in situ* Raman spectroscopy is also a powerful tool to monitor the degradation process.[20,29] Fig. S4a and b† show the stacked Raman spectra with increasing measurements under the irradiation of 0.2 mW and 2 mW in air, respectively. Similarly, several representative Raman modes ($A_1(\Gamma_1^2)$, $E(\Gamma_3^1)$-LO, and $A_1(\Gamma_1^3)$) of InSe all become weaker as the increasement of measurements no. for two situations. This indicates the integrity of the InSe layer destroyed by laser ablating, which provides a new proof for the degradation of InSe. It should be noted that the (178 cm^{-1} and 228 cm^{-1}) peaks almost disappear at the end of the test of 2 mW while two emergent broad brand individually located at ~133 cm^{-1} and ~200–250 cm^{-1} are detected, which has been proven to be good indicators of formation of oxidative products, such as amorphous In_2Se_3 and cubic In_2O_3 produced by a strong oxidation process in InSe.[30–33] These results are further in favor of the conclusion that the 2 mW irradiation can cause a severer oxidation in InSe relative to the 0.2 mW.

3.3 Three-dimensional (3D) AFM images of the InSe

In addition to these indirect strategies of spectroscopy, we also directly monitor the surface morphology of InSe in air through AFM measurement. Fig. 4a–f show the three-dimensional (3D) AFM images of the InSe in different test situations as well as the corresponding height profiles. As seen in the 3D images, after the laser irradiation of 0.2 mW, a minor pit formed on the surface, indicating the InSe can be slightly ablated with the presence of O_2 even at a low power. Notably, we find that the pit exhibits a noticeable increasement in diameter from measurement no. 5 to no. 40 according to the height profiles shown in Fig. 4d and e. Such behaviors demonstrate that the degrading effect induced by laser irradiation can be accumulated during the repeated measurements, which agrees well with the continuous decline of PL intensity (see Fig. 3a). In contrast, we observe a striking lump in a larger pit as shown in Fig. 4c where the InSe suffers a 2 mW irradiation, suggesting the InSe surface is seriously destroyed first and then new oxidation products are formed, which has been evidenced by the emergent broad brand in Raman spectra (see Fig. S4†). Specifically, the serious destruction should be attributed to the excess heat and intense oxidation, while the created oxidation products aggregate to form a protruding oxidation lump with the increase of measurements no. The AFM results present an intuitive proof for the degradation process of InSe, in good agreement with its PL weakening process. However, the reason for initial enhancement process of PL under 0.2 mW irradiation is hard to directly monitor through a technical means and still needs to be discussed in more depth. According to the analyses earlier in this work, we think that the passivation of Se vacancy induced by adsorption plays a dominant role for the enhancement of PL intensity. Although the degrading effect caused by laser may result in a suppression in PL, it is negligible compared to the promotion brought by passivation effect before reaching the saturation, which can be evidenced by the rapid rise (6

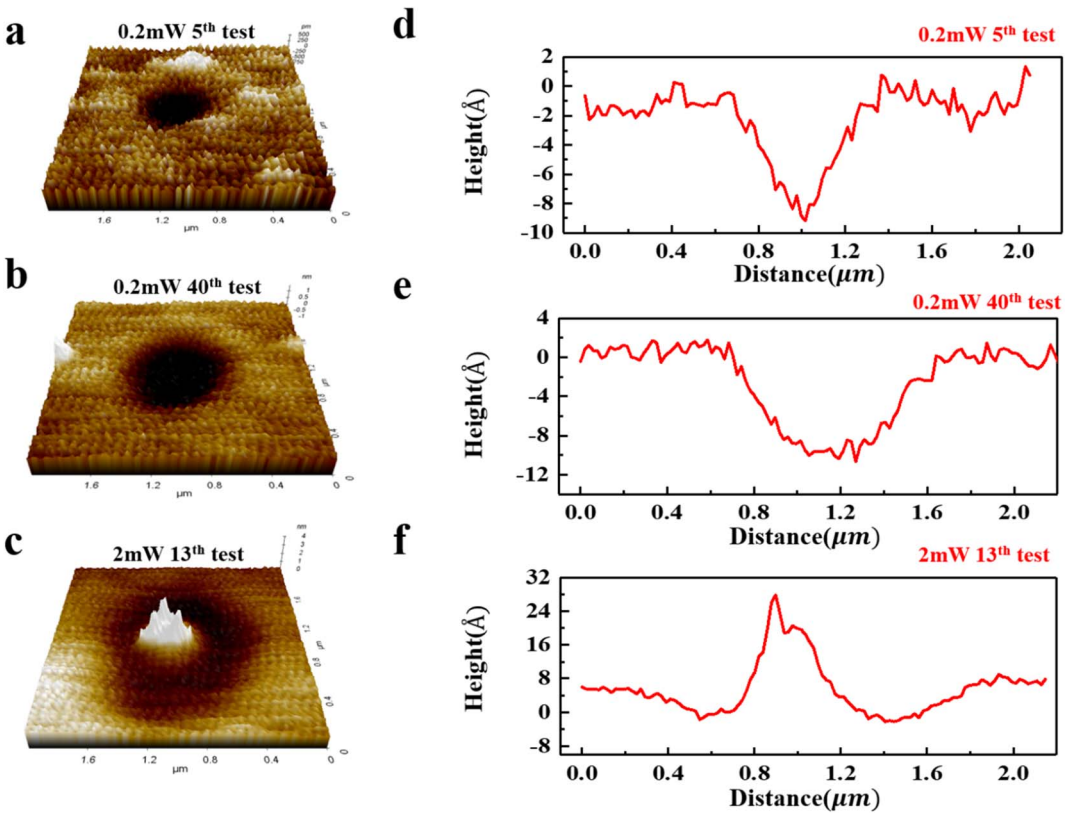

Fig. 4 (a–c) Three-dimensional (3D) AFM images of InSe during repeated measurement. (e–f) Corresponding height profiles.

measurements) and slow fall (~20 measurements) in PL intensity (see Fig. 3a).

3.4 The effect of vacancy density on the evolution of PL

It is well known that the PL emission intensity mainly depends on the radiative recombination efficiency while the non-radiative recombination is unavoidable in ambient, which might directly affect the PL intensity. According to previous reports, the vacancies[34,35] and atomic substitutions[36,37] existing in TMDs provide primary non-radiative recombination pathways and the former is considered to be the dominant structural defect on account of its low formation energy.[38,39] For InSe, first-principles calculation reveals that perfect InSe possesses high chemical stability against oxidation but intrinsic defects, like Se vacancies, can act as active sites for molecule adsorption,[10,40] which offers a possible path to enhance the PL emission by passivating the vacancies. In a similar way, the intrinsic Se vacancies in InSe flake will create certain mid-gap defect states that can act as a nonradiative recombination center, thus passivating these Se vacancies can effectively suppress non-radiative recombination to improve the PL emission efficiency. Theoretical calculations also demonstrate that light excitation can significantly accelerate the degeneration of InSe by forming chemical oxygen species[10] and the energy barrier of O_2 adsorbed on Se vacancies is much lower than on In vacancies.[9] This confirms the possibility of that O_2 occupy the Se vacancies under the irradiation of 0.2 mW and can account for the enhancement of PL.

Therefore, we expect to design an ingenious experiment to verify our opinion through investigating the effect of vacancy density on the evolution of PL in InSe. Slow energy argon (Ar) plasma treatment has been used as a nondestructive preconditioning technique to tailor the electrical and optical properties of TMDs.[41,42] On the other hand, mild Ar plasma is also often employed to controllably introduce vacancy in 2D system, for example, preferentially sputtering Se in 2D $PtSe_2$.[43,44] To this regard, we introduce different amounts of Se vacancies in InSe by changing Ar plasma treatment duration and show the corresponding Raman spectra of InSe in Fig. S5.† All the Raman modes are still detected after plasma treatment, indicating that the crystalline structure of InSe can be reserved. Interestingly, the $A_1(\Gamma_1^1)$-TO mode at 196 cm^{-1} changes more prominent after 60 s treatment which is normally forbidden and can be activated when near resonance happens or q-dependent scattering predominates.[45–47] The enhanced activity for $A_1(\Gamma_1^1)$-TO mode may result from the increased amount of Se vacancy introduced by plasma treatment.[28] Meanwhile, we also conduct the PL measurements of the plasma-treated InSe at ultralow temperature (10 K) to further confirm the reliability of introducing vacancies in InSe (see details in Fig. S6†).

The PL spectra of InSe flake treated by Ar plasma with different durations are recorded and shown in Fig. 5a. The PL intensity is obviously quenched, which might originate from the stronger non-radiative recombination induced by introducing more defects, such as vacancies.[44,48,49] We monitor the PL intensity evolution of plasma-treated InSe *versus* measurement no. under 0.2 mW irradiation as shown in Fig. 5b. A similar evolution to the untreated InSe is observed that the PL intensity firstly increases to the maximum value and then gradually decreases. In particular, we noticed that the maximum PL intensities of these plasma-treated InSe flakes are comparable to the pristine InSe after several irradiations, though their initial intensities are smaller. This phenomenon tells us that the PL efficiency of plasma-treated InSe could be well restored through a proper laser irradiation, which offers a good chance to study the effect of defect healing (*i.e.* vacancy passivation) on PL emission. It is noted that these similar maxima of PL also suggest there is a threshold for such enhancement behavior when all vacancies are eliminated.

In detail, we compare the increment of PL intensity induced by 0.2 mW irradiation in the InSe flake, in which the increment is defined as the difference between the initial and maximum value of PL. Fig. 5c gives the obtained PL increments with different treatment durations and the inset shows the ratio between the initial and maximum PL intensity values. As expected, we observe the strongest increment in the InSe flake with a 60 s treatment, there is no doubt that it has been introduced the most vacancies, which can be evidenced by its smallest initial PL intensity. Therefore, we can conclude that the observed PL enhancement of InSe under 0.2 mW irradiation is relative to the defect healing which means passivating vacancy by laser irradiation is an effective method to regulate the PL emission in InSe. On the other hand, we also monitor the PL intensity evolution of plasma-treated InSe as increasing measurements under 2 mW irradiation as shown in Fig. 5d. The PL intensities of these plasma-treated InSe decrease faster than the pristine InSe, demonstrating that more intense oxidation happened in InSe with higher defect density.

In general, we give a reasonable explanation for the PL evolutions of InSe induced by laser irradiation, which can be employed to act as an indicator of InSe degradation. Combining the discussion with previous studies,[9,10,17,26,34,35] we think that the vacancy passivation should be the primary reason for the enhancement process of PL in InSe where the H_2O and O_2 are adsorbed to the surface and occupy the Se vacancies under a weak laser irradiation, resulting in the decrease of the non-radiative recombination centers offered by related defect states. Meanwhile the direct adsorption of H_2O on the InSe surface is considered difficult but the atomic O group can dramatically enhance its adsorption ability according to the previous theoretical study,[10] our work experimentally confirms this opinion well based on the fact that the rich-water InSe exhibits the largest PL enhancement in air but not in vacuum. Moreover, the continuous decline of PL under 0.2 mW irradiation has been shown to come from the degrading effect of weak oxidation, however it should be attributed to the combination of excess heating and strong oxidation effect for the 2 mW irradiation. The possible oxidation process is that O_2 molecules become superoxide anions (O_2^-) under the irradiation of laser, reducing the dissociation barrier of O_2 and thus promoting the formation of the In–O structures in the Se-deficient InSe sheet.[10] It is worth noting that a weak oxidation process in InSe hardly produces any products but abundant oxidation products will be

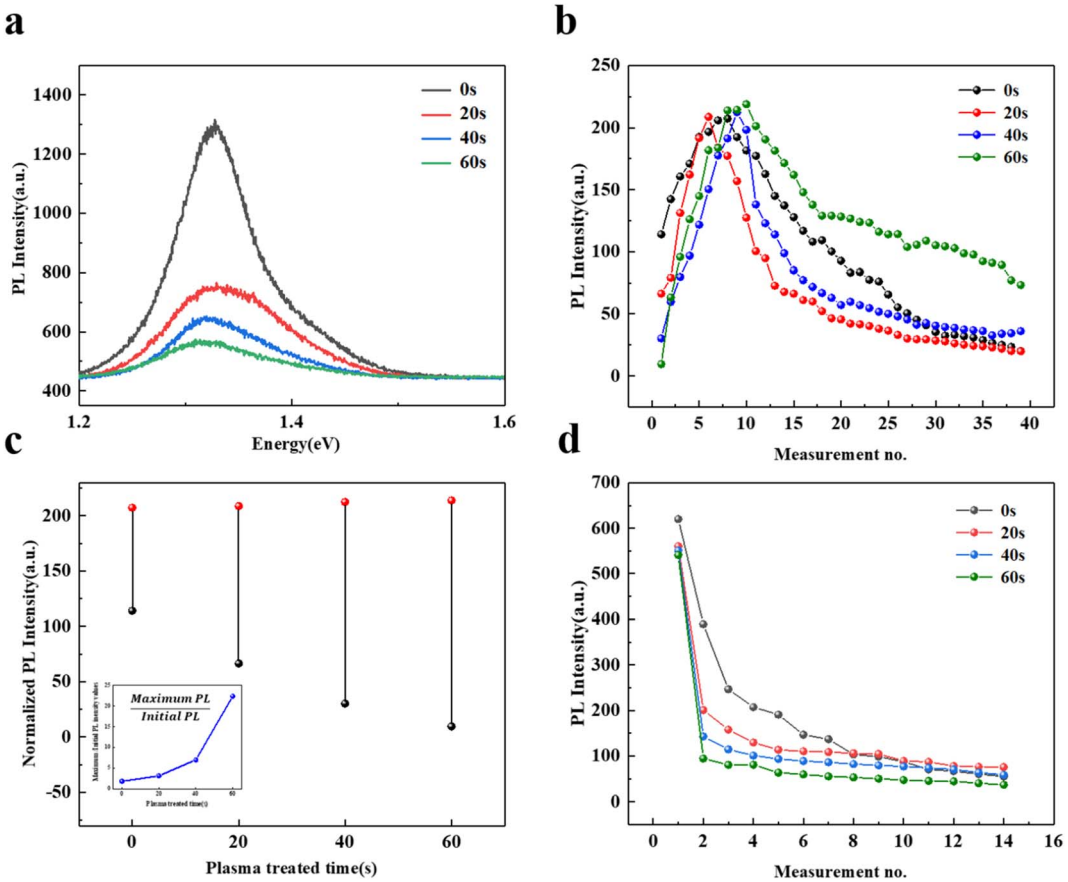

Fig. 5 (a) PL spectra of InSe treated with Ar plasma after 0 s, 20 s, 40 s, 60 s. (b) PL intensity under 0.2 mW laser irradiation as a function of measurement numbers (No.) after different duration of Ar plasma treatment. (c) PL increments (defined as the difference between the initial and maximum value of PL) after different duration of Ar plasma treatment. (d) PL intensity under 2 mW laser irradiation as a function of measurement numbers (No.) after different duration of Ar plasma treatment.

generated when the oxidation reaction is sufficiently intense, such as the 2 mW irradiation.

4. Conclusions

In summary, we systematically investigate the effect of laser irradiation on the InSe by monitoring the photo-induced evolution of PL. We find that weak laser irradiation enables the PL increase of InSe in air, however multiple irradiations or stronger power will result in a continuous decline. Such behavior means that we can achieve the regulation of InSe PL by simply manipulating the conditions of laser irradiation. Combining the AFM and Raman results, we clearly distinguish the roles of O_2, H_2O and intrinsic defects in the enhancement process of PL, while two different explanations for the PL decline are proposed, corresponding to that induced by the weak and strong irradiation, respectively. Interestingly, we also find that the vacancy passivation has a more visible effect on the PL of InSe compared to the weak oxidation, but the final saturation is not surprisingly observed. This work provides an experimental guidance for understanding InSe degradation and a reference for the application of environmentally stable InSe optoelectronic devices.

Author contributions

Jing Wang: methodology, investigation and write – original draft; Xiaofei Yue: improved the manuscript; Chunxiao Cong and Zhi-Jun Qiu conceptualization, supervision, funding acquisition.

Conflicts of interest

There are no conflicts to declare.

Acknowledgements

This research was supported by the Natural Science Foundation of China (no. 62074045 and 61774040), the National Key R&D Program of China (grant no. 2018YFA0703700), the Shanghai Municipal Natural Science Foundation (grant no. 20ZR1403200), and the National Young 1000 Talent Plan of China.

Notes and references

1 B. Radisavljevic, A. Radenovic, J. Brivio, V. Giacometti and A. Kis, *Nat. Nanotechnol.*, 2011, **6**, 147–150.

2 Q. J. Xiang, J. G. Yu and M. Jaroniec, *J. Am. Chem. Soc.*, 2012, **134**, 6575–6578.
3 A. Shokri and N. Salami, *Sens. Actuators, B*, 2016, **236**, 378–385.
4 T. H. Tsai, Z. Y. Liang, Y. C. Lin, C. C. Wang, K. I. Lin, K. Suenaga and P. W. Chiu, *ACS Nano*, 2020, **14**, 4559–4566.
5 E. Yoo, J. Kim, E. Hosono, H. Zhou, T. Kudo and I. Honma, *Nano Lett.*, 2008, **8**, 2277–2282.
6 D. A. Bandurin, A. V. Tyurnina, G. L. Yu, A. Mishchenko, V. Zolyomi, S. V. Morozov, R. K. Kumar, R. V. Gorbachev, Z. R. Kudrynskyi, S. Pezzini, Z. D. Kovalyuk, U. Zeitler, K. S. Novoselov, A. Patane, L. Eaves, I. V. Grigorieva, V. I. Fal'ko, A. K. Geim and Y. Cao, *Nat. Nanotechnol.*, 2017, **12**, 223–227.
7 M. Brotons-Gisbert, D. Andres-Peuares, J. Suh, F. Hidalgo, R. Abargues, P. J. Rodriguez-Canto, A. Segura, A. Cros, G. Tobias, E. Canadell, P. Ordejon, J. Q. Wu, J. P. Martinez-Pastor and J. F. Sanchez-Royo, *Nano Lett.*, 2016, **16**, 3221–3229.
8 G. W. Mudd, S. A. Svatek, T. Ren, A. Patane, O. Makarovsky, L. Eaves, P. H. Beton, Z. D. Kovalyuk, G. V. Lashkarev, Z. R. Kudrynskyi and A. I. Dmitriev, *Adv. Mater.*, 2013, **25**, 5714–5718.
9 D. W. Ma, T. X. Li, D. Yuan, C. Z. He, Z. W. Lu, Z. S. Lu, Z. X. Yang and Y. X. Wang, *Appl. Surf. Sci.*, 2018, **434**, 215–227.
10 A. A. Kistanov, Y. Cai, K. Zhou, S. V. Dmitriev and Y. W. Zhang, *J. Mater. Chem. C*, 2018, **6**, 518–525.
11 D. W. Ma, W. W. Ju, Y. A. Tang and Y. Chen, *Appl. Surf. Sci.*, 2017, **426**, 244–252.
12 X. Wei, C. F. Dong, A. N. Xu, X. G. Li and D. D. MacDonald, *Phys. Chem. Chem. Phys.*, 2018, **20**, 2238–2250.
13 A. Politano, G. Chiarello, R. Samnakay, G. Liu, B. Gurbulak, S. Duman, A. A. Balandin and D. W. Boukhvalov, *Nanoscale*, 2016, **8**, 8474–8479.
14 X. Wei, C. F. Dong, A. N. Xu and X. G. Li, *Appl. Surf. Sci.*, 2019, **475**, 487–493.
15 Y. Li, J. Yan, J. Chen, T. Yu, H. Ren, X. Liu, W. Liu, G. Yang, C. Xu, Q. Bao, Y. Liu and H. Xu, *Nano Res.*, 2021, **14**, 4274–4280.
16 H. M. Oh, G. H. Han, H. Kim, J. J. Bae, M. S. Jeong and Y. H. Lee, *ACS Nano*, 2016, **10**, 5230–5236.
17 X. X. Wei, Z. H. Yu, F. R. Hu, Y. Cheng, L. W. Yu, X. Y. Wang, M. Xiao, J. Z. Wang, X. R. Wang and Y. Shi, *AIP Adv.*, 2014, **4**, 123004.
18 P. Atkin, D. W. M. Lau, Q. Zhang, C. Zheng, K. J. Berean, M. R. Field, J. Z. Ou, I. S. Cole, T. Daeneke and K. Kalantar-Zadeh, *2D Mater.*, 2018, **5**, 015013.
19 S. V. Siyaram, A. T. Hanbicki, M. R. Rosenberger, G. G. Jernigan, H. J. Chuang, K. M. McCreary and B. T. Jonker, *ACS Appl. Mater. Interfaces*, 2019, **11**, 16147–16155.
20 S. F. Quan, Y. Y. Wang, J. Jiang, S. Y. Fu, Z. L. Li, Y. Liang, S. Guo, B. Zhong, K. Yu, H. Zhang and G. F. Kan, *J. Phys. Chem. C*, 2021, **125**, 25608–25614.
21 F. E. Faradev, N. M. Gasanly, B. N. Mavrin and N. N. Melnik, *Phys. Status Solidi B*, 1978, **85**, 381–386.
22 N. M. Gasanly, B. M. Yavadov, V. I. Tagirov and E. A. Vinogradov, *Phys. Status Solidi B*, 1978, **89**, K43–K48.
23 T. Zheng, Z. T. Wu, H. Y. Nan, Y. F. Yu, A. Zafar, Z. Z. Yan, J. P. Lu and Z. H. Ni, *RSC Adv.*, 2017, **7**, 54964–54968.
24 Y. H. Sun, S. L. Luo, X. G. Zhao, K. Biswas, S. L. Li and L. J. Zhang, *Nanoscale*, 2018, **10**, 7991–7998.
25 J. F. Sanchez-Royo, G. Munoz-Matutano, M. Brotons-Gisbert, J. P. Martinez-Pastor, A. Segura, A. Cantarero, R. Mata, J. Canet-Ferrer, G. Tobias, E. Canadell, J. Marques-Hueso and B. D. Gerardot, *Nano Res.*, 2014, **7**, 1556–1568.
26 S. Tongay, J. Zhou, C. Ataca, J. Liu, J. S. Kang, T. S. Matthews, L. You, J. B. Li, J. C. Grossman and J. Q. Wu, *Nano Lett.*, 2013, **13**, 2831–2836.
27 H. Y. Nan, Z. L. Wang, W. H. Wang, Z. Liang, Y. Lu, Q. Chen, D. W. He, P. H. Tan, F. Miao, X. R. Wang, J. L. Wang and Z. H. Ni, *ACS Nano*, 2014, **8**, 5738–5745.
28 H. Y. Nan, S. J. Guo, S. Cai, Z. R. Chen, A. Zafar, X. M. Zhang, X. F. Gu, S. Q. Xiao and Z. H. Ni, *Semicond. Sci. Technol.*, 2018, **33**, 074002.
29 A. Bergeron, J. Ibrahim, R. Leonelli and S. Francoeur, *Appl. Phys. Lett.*, 2017, **110**, 24.
30 C. Y. Wang, Y. Dai, J. Pezoldt, B. Lu, T. Kups, V. Cimalla and O. Ambacher, *Cryst. Growth Des.*, 2008, **8**, 1257–1260.
31 H. S. Kim, H. G. Na, J. C. Yang, C. Lee and H. W. Kim, *Acta Phys. Pol., A*, 2011, **119**, 143–145.
32 O. A. Balitskii, V. P. Savchyn and V. O. Yukhymchuk, *Semicond. Sci. Technol.*, 2002, **17**, L1–L4.
33 C. H. Ho, *Sci. Rep.*, 2014, **4**, 4764.
34 Y. Y. Liu, P. Stradins and S. H. Wei, *Angew. Chem., Int. Ed.*, 2016, **55**, 965–968.
35 S. Roy, W. Choi, S. Jeon, D. H. Kim, H. Kim, S. J. Yun, Y. Lee, J. Lee, Y. M. Kim and J. Kim, *Nano Lett.*, 2018, **18**, 4523–4530.
36 S. Barja, S. Refaely-Abramson, B. Schuler, D. Y. Qiu, A. Pulkin, S. Wickenburg, H. Ryu, M. M. Ugeda, C. Kastl, C. Chen, C. Hwang, A. Schwartzberg, S. Aloni, S. K. Mo, D. F. Ogletree, M. F. Crommie, O. V. Yazyev, S. G. Louie, J. B. Neaton and A. Weber-Bargioni, *Nat. Commun.*, 2019, **10**, 3382.
37 J. Peto, T. Ollar, P. Vancso, Z. I. Popov, G. Z. Magda, G. Dobrik, C. Y. Hwang, P. B. Sorokin and L. Tapaszto, *Nat. Chem.*, 2018, **10**, 1246–1251.
38 W. Zhou, X. L. Zou, S. Najmaei, Z. Liu, Y. M. Shi, J. Kong, J. Lou, P. M. Ajayan, B. I. Yakobson and J. C. Idrobo, *Nano Lett.*, 2013, **13**, 2615–2622.
39 K. C. Santosh, R. C. Longo, R. Addou, R. M. Wallace and K. Cho, *Nanotechnology*, 2014, **25**, 375703.
40 L. Shi, Q. H. Zhou, Y. H. Zhao, Y. X. Ouyang, C. Y. Ling, Q. Li and J. L. Wang, *J. Phys. Chem. Lett.*, 2017, **8**, 4368–4373.
41 A. D. Barbosa, C. A. D. Mendoza, Y. Lei, M. Giarola, M. Terrones, G. Mariotto and F. L. F. Junior, *Surf. Interfaces*, 2022, **33**, 102220.
42 M. Akhtaruzzaman, M. Shahiduzzaman, N. Amin, G. Muhammad, M. A. Islam, K. S. Bin Rafiq and K. Sopian, *Nanomaterials*, 2021, **11**, 1635.
43 X. F. Ping, D. Liang, Y. Y. Wu, X. X. Yan, S. X. Zhou, D. K. Hu, X. Q. Pan, P. F. Lu and L. Y. Jiao, *Nano Lett.*, 2021, **21**, 3857–3863.

44 M. Tosun, L. Chan, M. Amani, T. Roy, G. H. Ahn, P. Taheri, C. Carraro, J. W. Ager, R. Maboudian and A. Javey, *ACS Nano*, 2016, **10**, 6853–6860.
45 M. Zolfaghari, K. P. Jain, H. S. Mavi, M. Balkanski, C. Julien and A. Chevy, *Mater. Sci. Eng. B*, 1996, **38**, 161–170.
46 N. Kuroda, I. Munakata and Y. Nishina, *J. Phys. Soc. Jpn.*, 1982, **51**, 839–843.
47 N. Kuroda and Y. Nishina, *Solid State Commun.*, 1980, **34**, 481–484.
48 Z. T. Wu, Z. Z. Luo, Y. T. Shen, W. W. Zhao, W. H. Wang, H. Y. Nan, X. T. Guo, L. T. Sun, X. R. Wang, Y. M. You and Z. H. Ni, *Nano Res.*, 2016, **9**, 3622–3631.
49 Q. K. Qian, W. J. Wu, L. T. Peng, Y. X. Wang, A. M. Z. Tan, L. B. Liang, S. M. Hus, K. Wang, T. H. Choudhury, J. M. Redwing, A. A. Puretzky, D. B. Geohegan, R. G. Hennig, X. D. Ma and S. X. Huang, *ACS Nano*, 2022, **16**, 7428–7437.